

KIC 7524178 – an SU UMa-Type Dwarf Nova Showing Predominantly Negative Superhumps throughout Supercycle

Taichi KATO

Department of Astronomy, Kyoto University, Sakyo-ku, Kyoto 606-8502
tkato@kusastro.kyoto-u.ac.jp

and

Yoji OSAKI

Department of Astronomy, School of Science, University of Tokyo, Hongo, Tokyo 113-0033
osaki@ruby.ocn.ne.jp

(Received 201 0; accepted 201 0)

Abstract

We analyzed the Kepler long cadence data of KIC 7524178 (=KIS J192254.92+430905.4), and found that it is an SU UMa-type dwarf nova with frequent normal outbursts. The signal of the negative superhump was always the dominant one even during the superoutburst, in contrast to our common knowledge about superhumps in dwarf novae. The signal of the positive superhump was only transiently seen during the superoutburst, and it quickly decayed after the superoutburst. The frequency variation of the negative superhump was similar to the two previously studied dwarf novae in the Kepler field, V1504 Cyg and V344 Lyr. This is the first object in which the negative superhumps dominate throughout the supercycle. Nevertheless, the superoutburst was faithfully accompanied by the positive superhump, indicating that the tidal eccentric instability is essential for triggering a superoutburst. All the pieces of evidence strengthen the thermal-tidal instability as the origin of the superoutburst and supercycle, making this object the third such example in the Kepler field. This object had unusually small (~ 1.0 mag) outburst amplitude and we discussed that the object has a high mass-transfer rate close to the thermal stability limit of the accretion disk. The periods of the negative and positive superhumps, and that of the candidate orbital period were 0.07288 d (average, variable in the range 0.0723–0.0731 d), 0.0785 d (average, variable in the range 0.0772–0.0788 d) and 0.074606(1) d, respectively.

Key words: accretion, accretion disks — stars: dwarf novae — stars: novae, cataclysmic variables — stars: individual (KIC 7524178)

1. Introduction

Cataclysmic variables (CVs) are close binary systems consisting of a white dwarf and a red-dwarf secondary transferring matter via the Roche-lobe overflow [for a review, see Warner (1995)]. SU UMa-type dwarf novae are a class of CVs which show superoutbursts in addition to normal dwarf-nova outbursts. The most distinguishing feature of superoutbursts is the presence of superhumps (positive superhumps), whose periods are a few percent longer than the orbital period. The origin of the superhump is generally considered as the consequence of the growth of the tidal eccentric instability when the disk radius reaches the 3:1 resonance (Whitehurst 1988), and the increased tidal dissipation results in the long, bright superoutburst (Osaki 1989; Osaki 1996) [thermal-tidal instability (TTI) model]. Although the TTI model has been widely accepted, it has been challenged by an irradiation-induced mass-transfer model (e.g. Smak 1991; Smak 2004; Smak 2009) and a pure thermal instability model (e.g. Cannizzo et al. 2010). Quite recently, Osaki, Kato (2013a) demonstrated that the variation of the frequency of the negative superhumps, which have shorter periods than the orbital period and are considered as a result of a tilted disk (e.g.

Harvey et al. 1995; Patterson et al. 1997; Wood, Burke 2007), exactly reproduces the disk radius variation predicted by the TTI model.

KIC 7524178 (also referred to as KIS J192254.92+430905.4, hereafter KIS J1922) is a CV identified as an object with an H α emission (Scaringi et al. 2013). KIS J1922 showed relatively strong Balmer and HeI emission lines on a blue continuum (Scaringi et al. 2013). These emission lines were sharp, suggesting a low orbital inclination. We analyzed the long cadence (LC) public Kepler data (quarters 15 and 16) of this object and found that it is an SU UMa-type dwarf nova with short outburst intervals. What is most surprising was that negative superhumps were predominantly present even during the superoutburst. In this Letter, we report our analysis of the object and examine whether such an unusual phenomenon can be understood within the framework of the TTI model.

2. Data Analysis and Results

The data analysis was performed practically in the same way as in Osaki, Kato (2013a) and Osaki, Kato (2013c): we used two-dimensional Fourier analysis with and with-

out the Han window function, and least absolute shrinkage and selection operator (Lasso; Tibshirani 1996; Kato, Uemura 2012; Kato, Maehara 2013) for detecting periodic signals. We use P_{orb} and P_{SH} for the orbital period and superhump period, respectively. We introduce the fractional superhump excess in the frequency unit $\varepsilon^* \equiv 1 - P_{\text{orb}}/P_{\text{SH}}$. ε_+^* and ε_-^* represent ε^* for positive and negative superhumps, respectively.

As seen in the upper panel of figure 1, the Kepler data immediately indicates the pattern of a frequently outbursting SU UMa-type dwarf nova: the existence of numerous short outbursts and one long outburst. The results of the Fourier analysis are shown in figure 1. Astonishingly, the signal around the frequency 13.7–13.8 c/d persisted with almost the constant strength (in flux unit) throughout the Kepler observation. Since the frequency is variable, this signal cannot be the orbital period. Instead, the frequency gradually increased prior to the long outburst, and more rapidly decreased during the long outburst, reached the minimum after the long outburst and started to increase again gradually. This pattern of the frequency variation follows the same pattern of the persistent negative superhumps in V1504 Cyg (Osaki, Kato 2013a; Osaki, Kato 2013c) and V344 Lyr (Osaki, Kato 2013c). Furthermore, we could detect a transient signal around frequency 12.5–12.8 c/d during the long outburst (BJD 2456283–2456290). By analogy with V1504 Cyg and V344 Lyr, we identified this transient signal as the positive superhump. Thus the long outburst is indeed a superoutburst and this star is an SU UMa star.

The Lasso two-dimensional power spectrum is shown in figure 2. This analysis used two frequency windows covering the fundamental and the first harmonic and suppressed the signal at other frequencies. Both the fundamental and the first harmonic signals of the negative superhumps were clearly detected with frequency variations as will be discussed below. The positive superhump was detected as a broad band. The first harmonic was more strongly detected for the positive superhump due to strongly non-sinusoidal profile of the positive superhump.

3. Discussion

3.1. Frequency Variation of Negative Superhumps

The global frequency variation of the negative superhumps closely followed the pattern observed in V1504 Cyg and V344 Lyr. This global variation reflects the secular increase of the disk radius (and the angular momentum) with the progress of the supercycle. In addition to this, the frequency reached a local peak around the maximum of each normal outburst and then decreased during the subsequent fading. This pattern is also common to V1504 Cyg and V344 Lyr, and it reflects the variation of the disk radius due to the thermal instability.¹ In both re-

¹ Smak (2013) claimed that this interpretation is unjustifiable. We presented our detailed accounts to all of his criticisms by offering clear explanations to his criticisms in Osaki, Kato (2013b), and indicated that the variation of the disk radius most strongly affects the frequency variation of the negative superhumps. We

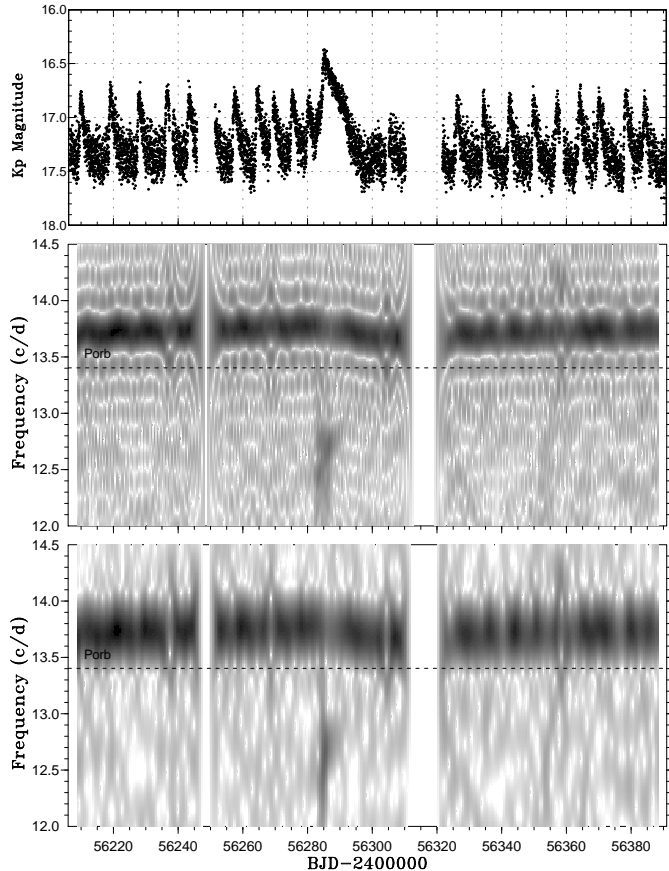


Fig. 1. Two-dimensional power spectrum of the Kepler long cadence light curve of KIS J1922. The orbital period (0.074606 d) estimated in subsection 3.4 is marked on the figure. (Upper:) Kepler Light curve. (Middle:) Power spectrum. The width of the sliding window and the time step used are 5 d and 0.5 d, respectively. No window function was used. (Lower) Power spectrum with Han window function. Although the side lobes are suppressed, the frequency resolution becomes lower.

spects, we can add yet another example supporting the TTI model.

The degree of variation of the frequency in accordance with the normal outburst is smaller in KIS J1922 than in V1504 Cyg and V344 Lyr [this becomes more apparent with the phase dispersion minimization (PDM; Stellingwerf 1978) analysis in subsection 3.4]. This can be understood as an effect of a shorter interval between normal outbursts in KIS J1922: the time for the disk to shrink is shorter in KIS J1922 (see a discussion in Osaki, Kato 2013b. for more potential factors). KIS J1922 resembles ER UMa and BK Lyn (Osaki, Kato 2013b). in the small degree of frequency variations in accordance with the normal outburst interval.

3.2. Profile of Negative Superhumps

The profile of negative superhumps in different phases is shown in figure 3. The profile tends to have a rather flat

followed this interpretation throughout this letter.

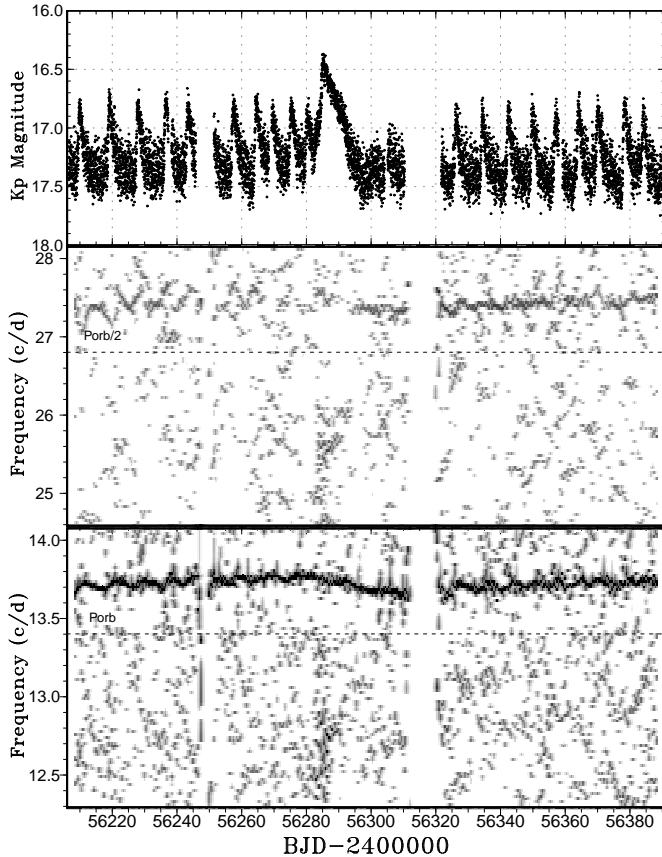


Fig. 2. Two-dimensional Lasso power spectrum of the Kepler long cadence light curve of KIS J1922. (Upper:) Kepler Light curve. (Middle:) Lasso power spectrum ($\log \lambda = -4.5$) of the first harmonic. The width of the sliding window and the time step used are 4 d and 0.5 d, respectively. The Lasso spectrum was obtained by assuming two frequency windows covering the fundamental and the first harmonic. The first harmonic component of the negative superhump is stronger in the earlier part of the supercycle (i.e., in the later part of the figure, especially after the superoutburst). The harmonic component of the positive superhump can be also seen. (Lower) Lasso power spectrum of the fundamental. The frequency variation of the negative superhump is very clearly depicted. The frequency gradually increased during a sequence of normal outbursts. The frequency also shows a variation in accordance with the normal outburst.

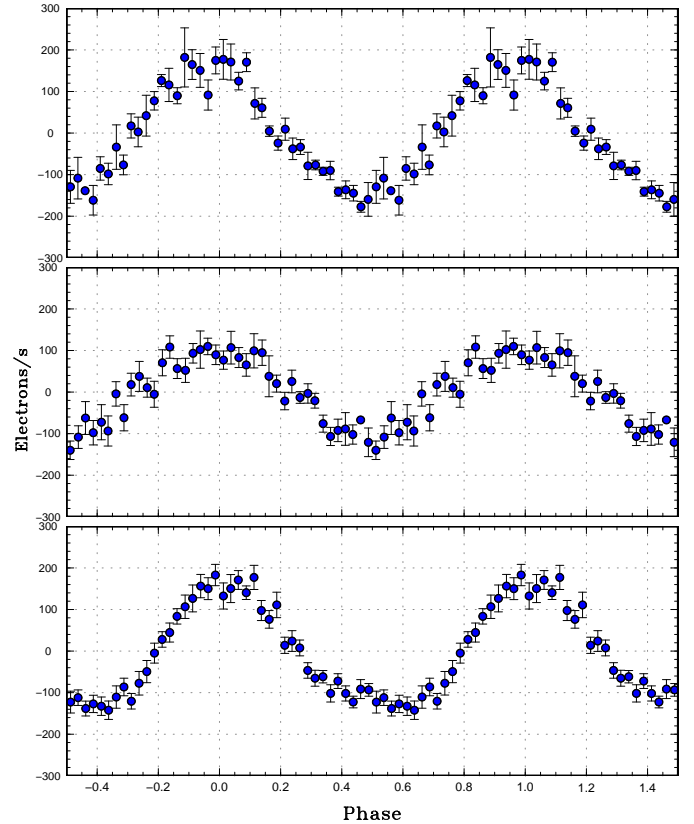


Fig. 3. Profile variation of negative superhumps in KIS J1922. (Upper:) Before the superoutburst (BJD 2456250–2456256, $P=0.07272$ d). (Middle:) During the superoutburst (BJD 2456285–2456292, $P=0.07281$ d). (Lower:) After the superoutburst (BJD 2456298–2456311, $P=0.07311$ d). The flux unit $1800 \text{ electrons s}^{-1}$ roughly corresponds to the Kepler magnitude of 17. For a 17.0-mag object, the relative amplitude of 200 electrons s^{-1} corresponds to an amplitude of 0.11 mag.

minimum and a slightly slower rise than the fade, all of which are common to the negative superhumps in V1504 Cyg (figure 6 in Osaki, Kato 2013c), although the asymmetry is less prominent in KIS J1922. This is probably because the disk in KIS J1922 always stays close to the hot state, and the profile may not vary strongly in accordance with the outburst state.

3.3. Positive Superhumps

As seen in figures 1 and 2, the positive superhumps were only briefly present during the superoutburst, and the strength of the signal of the negative superhumps always dominated over the positive superhumps. In ER UMa, negative superhumps were very prominently seen even during superoutbursts in 2011–2012 (Ohshima et al. 2012). Even in the case of ER UMa, the initial stage of the superoutbursts was dominated by the positive superhumps. KIS J1922 is the first object in which the negative superhump dominates throughout the supercycle. Nevertheless, there has been no exception to the rule that the positive superhumps always appear during the

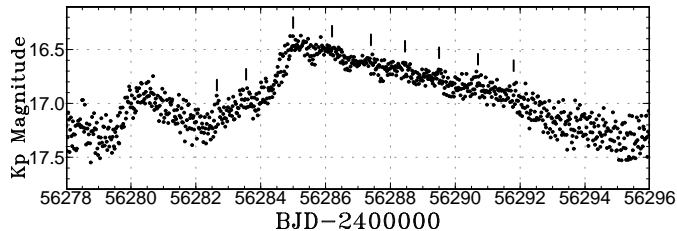


Fig. 4. Enlargement of the superoutburst. The maxima of the beat phenomenon between the positive and negative superhumps are labeled by the ticks.

superoutburst including the most extreme cases such as the object and ER UMa (Ohshima et al. 2012). We can conclude that the faithful existence of the positive superhumps during the superoutburst indicates that the tidal eccentric instability is essential for triggering a superoutburst, as predicted by the TTI theory.

By looking at the pattern of the beat phenomenon between the negative and positive superhumps in the light curve (figure 4), we could trace the development of the positive superhumps. The beat phenomenon with a period of ~ 1 d could be detected throughout the plateau part of the superoutburst with decreasing amplitudes. This suggests that the positive superhump were decaying during the plateau phase, and almost disappeared at the end of the plateau phase. This behavior is in agreement with the two-dimensional power spectral analysis, which has a lower time resolution. The beat phenomenon could be traced to the slowly rising part (BJD 2456283–2456285) just preceding the superoutburst. This suggests that the positive superhumps were growing just after the normal outburst preceding the superoutburst (i.e. stage A superhumps, Kato et al. 2009). The normal outburst was thus a precursor outburst as in V1504 Cyg (BJD 2455876–2455879, Osaki, Kato 2013b). The apparent lack of the precursor part in the main superoutburst (starting from BJD 2456285) can naturally be understood.

3.4. Estimation of Orbital Period

As shown in Osaki, Kato (2013c), ε_+^* is approximately $7/4$ times² larger than ε_-^* when the pressure effect can be ignored. By comparing the measured frequencies of negative and positive superhumps when both signals are simultaneously present, we can estimate the orbital period. Since the positive superhumps never became the dominant signal in KIS J1922, we consider that the eccentricity is almost confined to the outer edge of the disk and the pressure effect can be ignored (cf. Osaki, Kato 2013c). This relation was obtained when we assume an orbital period of 0.07455 ± 0.00010 d. We found a candidate orbital period (5σ detection) of $0.074606(1)$ d in this period range using the entire LC data (figure 5). This period well explains the relation between ε_+^* and ε_-^* (figure 6) as in V1504 Cyg and V344 Lyr (Osaki, Kato 2013c).

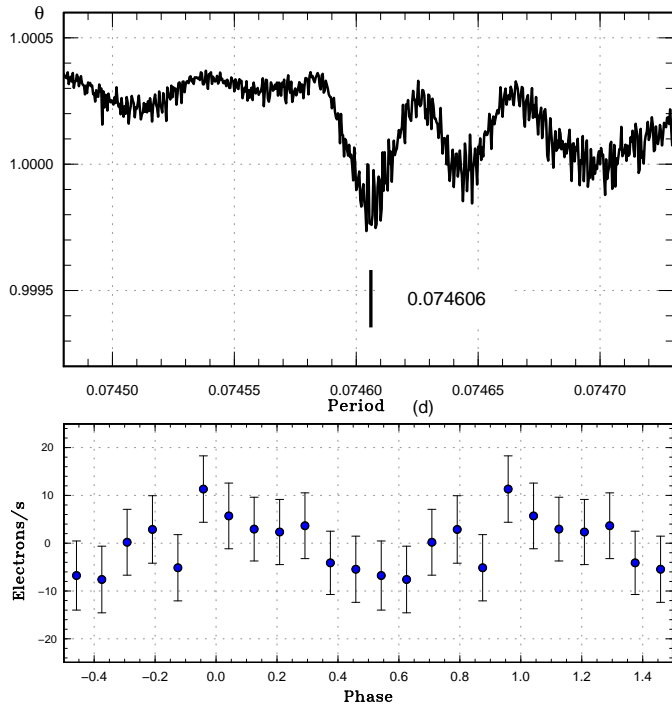


Fig. 5. Possible orbital period. (Upper:) PDM analysis. (Lower:) Phase-averaged light curve.

This candidate orbital period appears to be sometimes present in the Lasso spectrum (figure 2). The weakness of the signal of the orbital period is consistent with the low orbital inclination suggested from the spectrum.

Assuming this orbital period, we can estimate the mass ratio ($q = M_2/M_1$) by the method of Kato, Osaki (2013). Since the positive superhump grew (stage A superhumps) during BJD 2456281–2456285, we used the frequency of this interval [$12.77(2)$ c/d] and obtained $q=0.14(1)$. The minimum frequency [$12.68(2)$ c/d] was recorded in the segment BJD 2456284–2456288. This frequency corresponds to $q=0.16(1)$. Considering the uncertainties in the frequency determination, we estimated q to be in a range of 0.14 – 0.16 .

3.5. Cycle Length and Estimated Supercycle

The intervals between the normal outbursts ranged from 5–9 d, the shortest ones were seen just before the superoutburst. The cycle length is thus between the extreme ER UMa-type objects (cycle lengths as short as 4 d; Kato, Kunjaya 1995; Robertson et al. 1995; Patterson et al. 1995) and SU UMa-type dwarf novae with shortest cycle lengths such as YZ Cnc (8 d).

Although only one superoutburst was recorded in the Kepler data, we can estimate the supercycle length by using the systematic slow increase of the frequency of the negative superhump as supercycle phase increases. A supercycle of $140(10)$ d produces a smooth frequency variation versus the supercycle phase before and after the superoutburst, and we expect that the supercycle length of

² This value is weakly dependent on the distribution of the mass in the disk, see appendix in Osaki, Kato (2013c).

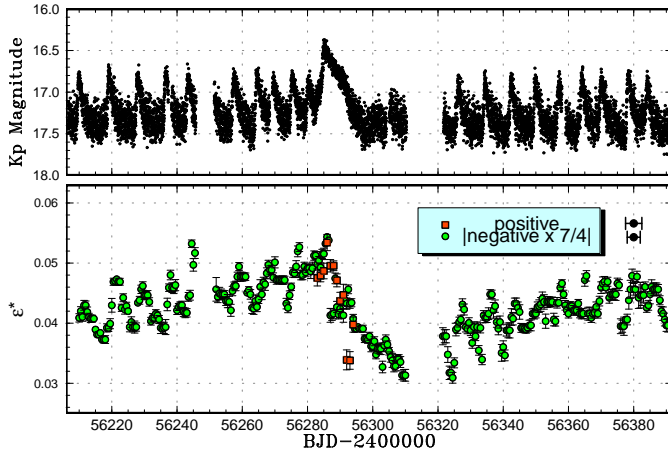


Fig. 6. Variation in precession rates of positive and negative superhumps given by two ϵ^* 's of KIS J1922 assuming an orbital period of 0.074606 d. (Upper:) Light curve. (Lower:) Absolute values of fractional superhump excesses (positive and negative) in frequency scale determined by the PDM method. The window widths (5 d and 4 d for the positive and negative superhumps, respectively; a longer width was adopted for the positive superhumps due to the weakness of the signal) are indicated by horizontal bars at the upper right corner and the error bars represent 1σ errors in the frequencies.

KIS J1922 is around this value. This supercycle length is slightly longer than those of V1504 Cyg [115(1) d] and V344 Lyr [114(1) d].

3.6. Short Duration of Superoutburst

The duration of plateau portion of the superoutburst was only 7 d (BJD 2456285–2456292), which is much shorter than those (10–14 d) of most of SU UMa-type dwarf novae. The case appears similar to ER UMa (Ohshima et al. 2012), in which the duration of the superoutburst is shorter when negative superhumps appeared. This consequence is naturally understood assuming a disk tilt. If the disk is tilted, the gas stream from the secondary reaches the inner part of the accretion disk and thereby reduces the mass-transfer rate in the outer part of the disk, which is responsible for a long-duration superoutburst in high mass-transfer systems (Osaki 1995).

In addition to this, the positive superhumps appear to be suppressed in the presence of the strong negative superhumps. While in most of SU UMa-type dwarf novae, including ER UMa stars, the signal of positive superhumps can survive for one or two cycles of normal outbursts (e.g. Patterson et al. 1995; Still et al. 2010; Osaki, Kato 2013c), the positive superhump disappeared soon after the plateau phase in KIS J1922. It appears that the disk tilt may somehow suppress the tidal eccentric instability, and this possibility deserves further investigation.

3.7. Low Outburst Amplitude

Although Kepler has no fixed zero points, the object was always recorded above 800 count s^{-1} , suggesting that

the amplitude of this dwarf nova is unusually low. The full amplitude in the Kepler data only amounted to 1.0 mag. The object was listed as an object with a g -magnitude of 16.61 in the Kepler Input Catalog and faintest magnitude recorded in the past survey plates was $B=18.35$ (USNO YB6 Catalog, unpublished, referred in NOMAD Catalog). The majority of the past records suggests that the object varied within a narrow range of 16.2–17.3 mag (system close to V), confirming the very low outburst amplitudes in Kepler observations. There is no contaminating object brighter than magnitude 19 within $15''$ of the object. An examination of the Digitized Sky Survey could not resolve any close companion. Considering that the object is faint in the infrared ($J=16.94$ and $K_s=17.27$ in 2MASS) and the $V-J$ color is consistent with a CV disk, we consider this light comes from the accretion disk, rather than an unresolved companion.

The low amplitude suggests that the accretion disk does not fully return to the true quiescent state (low state) and the some part of the disk always remains hot.

3.8. Cycle Length of Normal Outbursts

Osaki, Kato (2013a), Ohshima et al. (2012), Zemko et al. (2013) indicated that the presence of negative superhumps suppresses the occurrence of normal outbursts. This appears to be a reasonable consequence if the disk is indeed tilted: the mass supply to the outer disk is reduced and outside-in type outburst is expected to be suppressed. However, in the case of KIS J1922, the cycle length is as short as 5–9 d, and all normal outbursts appear to be outside-in type accompanied by a rapid rise (in ~ 1 d). This may be understood if the mass-transfer rate in KIS J1922 is close to the thermal stability, and the disk stays only slightly below the thermal stability. In such a system, the normal outbursts could occur more frequently (with intervals as short as 4 d) as in ER UMa stars, and the cycle length of 5–9 d may reflect the reduced occurrence of normal outbursts in the presence of a disk tilt. The condition appears to be close to BK Lyn (see also subsection 3.1). If the disk in KIS J1922 ceases to tilt, the object may enter the novalike state as in BK Lyn (cf. Kato et al. 2013).

Only a few systems below the period gap have (nearly) thermally stable disks. The well-known examples include BK Lyn (cf. Patterson et al. 2013) and post-novae such as V1974 Cyg (Skillman et al. 1997). BK Lyn has recently been proposed to be a post-outburst nova (Hertzog 1986; Patterson et al. 2013), suggesting that all these high mass-transfer objects below the period gap are post-outburst novae. Given the unusual nature of KIS J1922, a search for a nova remnant (cf. Shara et al. 2012a; Shara et al. 2012b) may be fruitful.

We thank the Kepler Mission team and the data calibration engineers for making Kepler data available to the public. This work was supported by the Grant-in-Aid “Initiative for High-Dimensional Data-Driven Science through Deepening of Sparse Modeling” from the Ministry of Education, Culture, Sports, Science and Technology

(MEXT) of Japan.

References

- Cannizzo, J. K., Still, M. D., Howell, S. B., Wood, M. A., & Smale, A. P. 2010, *ApJ*, 725, 1393
- Harvey, D., Skillman, D. R., Patterson, J., & Ringwald, F. A. 1995, *PASP*, 107, 551
- Hertzog, K. P. 1986, *Observatory*, 106, 38
- Kato, T., et al. 2013, *PASJ*, submitted
- Kato, T., et al. 2009, *PASJ*, 61, S395
- Kato, T., & Kunjaya, C. 1995, *PASJ*, 47, 163
- Kato, T., & Maehara, H. 2013, *PASJ*, 65, 76
- Kato, T., & Osaki, Y. 2013, *PASJ*, in press (arXiv astro-ph/1307.5588)
- Kato, T., & Uemura, M. 2012, *PASJ*, 64, 122
- Ohshima, T., et al. 2012, *PASJ*, 64, L3
- Osaki, Y. 1989, *PASJ*, 41, 1005
- Osaki, Y. 1995, *PASJ*, 47, L11
- Osaki, Y. 1996, *PASP*, 108, 39
- Osaki, Y., & Kato, T. 2013a, *PASJ*, 65, 50
- Osaki, Y., & Kato, T. 2013b, *PASJ*, submitted
- Osaki, Y., & Kato, T. 2013c, *PASJ*, in press (arXiv astro-ph/1305.5877)
- Patterson, J., Jablonski, F., Koen, C., O'Donoghue, D., & Skillman, D. R. 1995, *PASP*, 107, 1183
- Patterson, J., Kemp, J., Saad, J., Skillman, D. R., Harvey, D., Fried, R., Thorstensen, J. R., & Ashley, R. 1997, *PASP*, 109, 468
- Patterson, J., et al. 2013, *MNRAS*, 434, 1902
- Robertson, J. W., Honeycutt, R. K., & Turner, G. W. 1995, *PASP*, 107, 443
- Scaringi, S., Groot, P. J., Verbeek, K., Greiss, S., Knigge, C., & K rding, E. 2013, *MNRAS*, 428, 2207
- Shara, M. M., Mizusawa, T., Wehinger, P., Zurek, D., Martin, C. D., Neill, J. D., Forster, K., & Seibert, M. 2012a, *ApJ*, 758, 121
- Shara, M. M., Mizusawa, T., Zurek, D., Martin, C. D., Neill, J. D., & Seibert, M. 2012b, *ApJ*, 756, 107
- Skillman, D. R., Harvey, D., Patterson, J., & Vanmunster, T. 1997, *PASP*, 109, 114
- Smak, J. 2004, *Acta Astron.*, 54, 221
- Smak, J. 2009, *Acta Astron.*, 59, 121
- Smak, J. 2013, *Acta Astron.*, 63, 109
- Smak, J. I. 1991, *Acta Astron.*, 41, 269
- Stellingwerf, R. F. 1978, *ApJ*, 224, 953
- Still, M., Howell, S. B., Wood, M. A., Cannizzo, J. K., & Smale, A. P. 2010, *ApJL*, 717, L113
- Tibshirani, R. 1996, *J. R. Statist. Soc. B*, 58, 267
- Warner, B. 1995, *Cataclysmic Variable Stars* (Cambridge: Cambridge University Press)
- Whitehurst, R. 1988, *MNRAS*, 232, 35
- Wood, M. A., & Burke, C. J. 2007, *ApJ*, 661, 1042
- Zemko, P., Kato, T., & Shugarov, S. 2013, *PASJ*, 65, 54